Proceedings of the 2006 American Control Conference
Minneapolis, Minnesota, USA, June 14-16, 2006

Capture Regions of GIPN Guidance Laws: A Least Square SVM Approach

Feng Tyan
Computational Dynamics and Control Lab
Dept. of Aerospace Engineering
Tamkang University
Tamshui, Taipei County, Taiwan 25147, R. O. C.

***Abstract*— In this paper, the expression of capture region of the general ideal proportional navigation (GIPN) missile guidance law is determined by a powerful classifier, least square support vector machine (LSSVM). To reduce the computational burden, an approximation of the Gaussian radial basis function is adopted to obtain the corresponding nonlinear feature mapping function. Through numerous numerical examples, it shows that the proposed technique is adequate for the determination of capture region. All the analysis of the relative dynamics between missile and target are performed in a line of sight (LOS) fixed natural coordinate. To have the capture region ready for LSSVM, all the state variables are transformed into the modified polar variables form. In addition, to reduce the number of independent variables, these modified polar variables are further non-dimensionalized. For simplicity, we assume that target's input acceleration is subject to independent saturation, while missile's input acceleration is subject to magnitude saturation.**

I. Introduction

Although three-dimensional missile guidance have been widely used and studied in the guidance literature as was pointed out in [1] and the reference therein. Deriving the related capture condition is still one of the main topics being discussed [2–9]. However, only a few papers discussed capturability of guidance law in 3D space, and the result was either restricted to unbounded maneuvering target (True proportional navigation guidance law was considered) [8], or missile (guided by a Pure proportional navigation guidance law) is required to be launched toward the target [9]. In the author's previous work [10], the bounded maneuverability of missile utilizing General IPN guidance was considered, and the related capture region was determined graphically mainly. In this paper, the capture region for a nonmaneuvering target and missile with bounded maneuverability is derived. However, at this point, it is still hard to determine the capture region for a maneuvering target analytically. Hence, we resort to a powerful tool, support vector machine (SVM), to determine the capture region numerically so that it can be integrated with the onboard fire control computer.

Since its being introduced in 1995 [11], SVMs have been successfully implemented to a number of applications ranging from particle identification, face identification, and text categorization etc.. Classification is achieved by mapping input data into a high dimensional feature space where it may become linearly separable. Despite its many successful applications, most of the SVM algorithms are suffered from the expensive computational time and size of matrices involved in the training process for large scale problems. To remedy this, a least square SVM type algorithm was proposed by Chua [12]. In this algorithm the Sherman-Morrison-Woodbury (SMW) matrix identity is utilized to reduce the size of a matrix involved in inversion. However, to let LSSVM be computational efficient via the SMW identity, a kernel function related nonlinear feature mapping function is required, although this is not necessary for most of the other schemes. In this work, a Taylor's series approximation of the Gaussian radial basis kernel function is adopted for obtaining the related mapping function.

This paper is organized as follows. At first, the equations of motion for the relative dynamics between missile and target are derived in a LOS fixed natural coordinate, then transformed into the form in terms of modified polar variables (MPVs) [10] in section II. In addition, to reduce the number of independent variables these modified polar variables are further non-dimensionalized. Since the maneuverabilities of both missile and target are modelled by saturation functions, an analysis of saturation function is conducted in section III. For simplicity, we assume that target and missile input acceleration are subject to independent and magnitude saturation, respectively. Then the capture region of the GIPN missile guidance law is determined by the LSSVM in section V. After that some examples are tested to verify the proposed finite dimensional approximation of radial basis kernel function. Finally, a few conclusions are drawn.

II. Dynamic Equations in LOS Fixed Coordinate

Let the relative position vector r, i.e. line of sight (LOS), between target and missile be defined as (See Fig. 1)

$$r = r_T - r_M = \rho e_r, \tag{2.1}$$

where r_T and r_M are the position vectors of target and missile in an inertial coordinate $OXYZ$ respectively, ρ is the range between target and missile. Then the relative velocity

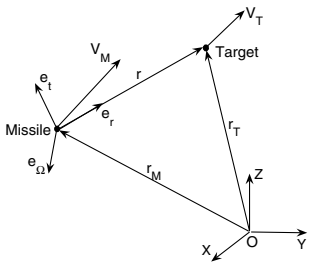

Fig. 1. Engagement geometry

and acceleration can be written as

$$\frac{d}{dt}r = v_r = \dot{\rho}e_r + \rho\dot{e}_r = v_T - v_M, \tag{2.2a}$$

$$\frac{d}{dt}v_r = \ddot{\rho}e_r + 2\dot{\rho}\dot{e}_r + \rho\ddot{e}_r = a_T - a_M, \tag{2.2b}$$

where e_r is a unit vector in the direction of the LOS, v_T, v_M and a_T, a_M stand for target and missile velocity and acceleration vectors respectively.

Assuming that the angular velocity of line of sight, Ω, is orthogonal to the line of sight, we have

$$\Omega = e_r \times \dot{e}_r = e_r \times (\Omega \times e_r). \tag{2.3}$$

It follows that

$$\dot{e}_r^{\mathrm{T}}\dot{e}_r = \|\Omega\|^2. \tag{2.4}$$

For convenience, let us define the following unit vectors

$$e_t \triangleq \frac{\dot{e}_r}{\|\Omega\|},\ e_\Omega \triangleq \frac{\Omega}{\|\Omega\|}. \tag{2.5}$$

Apparently (e_r, e_t, e_Ω) constitutes a line of sight fixed, right-handed coordinate system.

If the accelerations of target and missile, a_T and a_M, are expressed in the (e_r, e_t, e_Ω) coordinate system as

$$a_T \triangleq a_{Tr}e_r + a_{Tt}e_t + a_{T\Omega}e_\Omega,$$
$$a_M \triangleq a_{Mr}e_r + a_{Mt}e_t + a_{M\Omega}e_\Omega,$$

it can be shown that the equations of motion for the relative dynamics are

$$\begin{aligned}
&\frac{d}{dt}\dot{\rho} = \rho\|\Omega\|^2 + a_{Tr} - a_{Mr}, \dot{\rho}(t_0) = \dot{\rho}_0,\\
&\frac{d}{dt}\rho\|\Omega\| = -\dot{\rho}\|\Omega\| + a_{Tt} - a_{Mt}, \|\Omega(t_0)\| = \|\Omega_0\|,\\
&\frac{d}{dt}\rho = \dot{\rho}, \rho(t_0) = \rho_0.
\end{aligned} \tag{2.6}$$

However, to decouple the state ρ from the first two differential equations in (2.6), we introduce the following modified polar variables (MPVs) [10],

$$\begin{bmatrix} u \\ v \\ w \end{bmatrix} \triangleq \begin{bmatrix} \frac{\dot{\rho}}{\sqrt{\rho}} \\ \sqrt{\rho}\|\Omega\| \\ \sqrt{\rho} \end{bmatrix}, \begin{bmatrix} u(t_0) \\ v(t_0) \\ w(t_0) \end{bmatrix} = \begin{bmatrix} u_0 \\ v_0 \\ w_0 \end{bmatrix}. \tag{2.7}$$

To further reduce the dependence of the number of initial conditions, let us introduce the following dimensionless variables

$$\bar{u} \triangleq \frac{u}{V_0}, \bar{v} \triangleq \frac{v}{V_0}, \bar{w} \triangleq \frac{w}{w_0}, \tag{2.8}$$

where $V_0 \triangleq \sqrt{u_0^2 + v_0^2}$, and the corresponding independent variable

$$ds = \frac{V_0}{w_0}\frac{dt}{\bar{w}}. \tag{2.9}$$

In addition, let us define the "pseudo-dimensionless" accelerations

$$\bar{a}_M \triangleq \frac{a_M}{V_0^2},\ \bar{a}_T \triangleq \frac{a_T}{V_0^2}, \tag{2.10}$$

and the corresponding components

$$\bar{a}_{Mi} \triangleq \frac{a_{Mi}}{V_0^2},\ \bar{a}_{Ti} \triangleq \frac{a_{Ti}}{V_0^2}, i = r, t, \Omega. \tag{2.11}$$

Obviously, equation (2.6) can be transformed into the following form

$$\frac{d\bar{u}}{ds} = -\frac{1}{2}\bar{u}^2 + \bar{v}^2 + \bar{a}_{Tr} - \bar{a}_{Mr}, \tag{2.12a}$$

$$\frac{d\bar{v}}{ds} = -\frac{3}{2}\bar{u}\bar{v} + \bar{a}_{Tt} - \bar{a}_{Mt}, \tag{2.12b}$$

$$\frac{d\bar{w}}{ds} = \frac{1}{2}\bar{u}\bar{w}, \tag{2.12c}$$

with initial conditions

$$\bar{u}_0 \triangleq \bar{u}(s_0) = \frac{u_0}{V_0},\ \bar{v}_0 \triangleq \bar{v}(s_0) = \frac{v_0}{V_0},\ \bar{w}_0 \triangleq \bar{w}(s_0) = 1.$$

Note that $(\bar{u}_0, \bar{v}_0)$ constitutes the upper part of the unit circle,

$$\bar{u}_0^2 + \bar{v}_0^2 = 1,\ -1 \le \bar{u}_0 < 1,\ 0 \le \bar{v}_0 \le 1. \tag{2.13}$$

In this paper, we adopt the following definition for "capture region".

Definition 2.1: The Capture region $(\mathcal{CR})$ is the region in the $(\bar{u}, \bar{v})$-plane, such that if the initial condition $(\bar{u}_0, \bar{v}_0) \in \mathcal{CR}$ and along with a proper choice of navigation constants, for a predefined value ρ_f there exists a finite s_f such that

$$\bar{w}_f \triangleq \bar{w}(s_f) < \sqrt{\frac{\rho_f}{\rho_0}}. \tag{2.14}$$

III. Saturation Nonlinearities

For real scenarios, target and missiles are all subject to bounded maneuverabilities. In this work, we assume that target's acceleration is limited by independent saturation function, while missile's acceleration is bounded by magnitude saturation function. To take into account these inherited limitations, define the commanded accelerations for target and missile as

$$A_T = \sum_{i=r,t,\Omega} A_{Ti}e_i, A_M = \sum_{i=r,t,\Omega} A_{Mi}e_i,$$

respectively, and let the corresponding input accelerations be

$$a_T = \mathrm{sat}_I[A_T] = \sum_{i=r,t,\Omega} \mathrm{sat}_{(a_{Ti\min}, a_{Ti\max})}(A_{Ti})e_i,$$

$$a_M = \mathrm{sat}_M[A_M] = \mathrm{sat}_{(0, \frac{a_{M\ \max}}{A_M})}(1) \sum_{i=r,t,\Omega} A_{Mi}e_i,$$

where $\mathrm{sat}_I[\cdot], \mathrm{sat}_M[\cdot]$ stand for independent and magnitude saturation functions respectively, $\mathrm{sat}_{(L,U)}(\cdot) \triangleq \min(\max(\ \cdot\ , L), U)$, where L and U are the lower and upper bounds, $a_{Ti\max}, a_{Ti\min}$ are the upper and lower bounds of

saturation levels of a_{Ti} respectively, $\|\cdot\|$ stands for the Euclidian norm of a vector, $\|a_M\|_{\max}$ is the magnitude bound of a_M. Hence, we have

$$a_{Ti} = \text{sat}_{(a_{Ti\min}, a_{Ti\max})}(A_{Ti}), i = r, t, \Omega, \tag{3.1}$$

$$a_{Mi} = \text{sat}_{(0, \frac{a_{M\ \max}}{A_M})}(1) \cdot A_{Mi}, i = r, t, \Omega,$$
$$\triangleq \begin{cases} \min(1, \frac{\|a_M\|_{\max}}{\|A_M\|}) \cdot A_{Mi}, & \|A_M\| \neq 0 \\ 0, & \|A_M\| = 0 \end{cases}. \tag{3.2}$$

The scaling factor in the magnitude saturation function is defined as

$$\kappa(\|a_M\|_{\max}, \|A_M\|) \triangleq \text{sat}_{(0, \frac{a_{M\ \max}}{A_M})}(1),$$

hence, $0 < \kappa \leq 1$. A compact expression for κ is

$$\kappa = \min\left(1, \frac{\|a_M\|_{\max}}{\|A_M\| + \varepsilon}\right), \tag{3.3}$$

where $0 < \varepsilon \ll 1$. For simplicity, we omit the ε hereafter.

For notational convenience, let us define

$$\bar{A}_M \triangleq \frac{A_M}{V_0^2},\ \bar{A}_T \triangleq \frac{A_T}{V_0^2}, \tag{3.4}$$

and the related components

$$\bar{A}_{Mi} \triangleq \frac{A_{Mi}}{V_0^2},\ \bar{A}_{Ti} \triangleq \frac{A_{Ti}}{V_0^2}, i = r, t, \Omega, \tag{3.5}$$

along with their bounds

$$\|\bar{a}_M\|_{\max} \triangleq \frac{\|a_M\|_{\max}}{V_0^2},\ \bar{a}_{Ti\max} \triangleq \frac{a_{Ti\max}}{V_0^2}, i = r, t, \Omega.$$

The following lemmas allows us to write the saturation function in the equations of motion as a function of normalized variables.

Lemma 3.1: The scaling factor for magnitude saturation and the independent saturation remain unchanged under normalization, that is,

$$\kappa(\|a_M\|_{\max}, \|A_M\|) = \kappa(\|\bar{a}_M\|_{\max}, \|\bar{A}_M\|),$$
$$\frac{1}{V_0^2}\text{sat}_{(a_{Ti\min}, a_{Ti\max})}(A_{Ti}) = \text{sat}_{(\bar{a}_{Ti\min}, \bar{a}_{Ti\max})}(\bar{A}_{Ti}).$$

Hence, without causing any ambiguity we are going to omit the arguments of κ hereafter. As a result, the components of each pseudo-dimensionless acceleration are

$$\bar{a}_{Ti} = \text{sat}_{(\bar{a}_{Ti\min}, \bar{a}_{Ti\max})}(\bar{A}_{Ti}),\ \bar{a}_{Mi} = \kappa\bar{A}_{Mi}, i = r, t, \Omega.$$

IV. Missile and Target Input Accelerations

A. Unbounded a_M with Known a_T

For comparison and completeness, at first we consider the case when the target acceleration a_T is known and the magnitude of missile's acceleration a_M is unbounded. Let the missile commanded acceleration be

$$A_M = a_T + [\beta\dot{\rho}e_r + \alpha\rho\|\Omega\|e_t] \times \Omega. \tag{4.1}$$

The adopted name "GIPN" is used to emphasize that the bias angle between A_M and the normal direction of LOS is allowed, however it is varying with states instead of being fixed as proposed by Yuan [13].

Theorem 4.1: If the missile acceleration is

$$a_M = A_M = a_T + [\beta\dot{\rho}e_r + \alpha\rho\|\Omega\|e_t] \times \Omega, \tag{4.2}$$

Let the capture condition be $\rho(t_f) \leq \rho_f$, then the capture regions are given as follows:

1) For the case of $\alpha > 1$, it is necessary and sufficient that $\beta \geq 1$ and $\mathcal{CR}$ is defined as

$$\mathcal{CR} = \left\{(\bar{u}_0, \bar{v}_0)| -1 \leq \bar{u}_0 < 1, \bar{v}_0 = \sqrt{1 - \bar{u}_0^2}\right\} \tag{4.3}$$

2) If $\beta > 1$ and $\alpha \leq 1$, it is necessary and sufficient that

$$\mathcal{CR} = \left\{(\bar{u}_0, \bar{v}_0)\left|\frac{(1-\alpha)\bar{v}_0^2}{(\beta-1)\bar{u}_0^2}\left[1 - \left(\frac{\rho_f}{\rho_0}\right)^{2(\beta-1)}\right] < 1,\right.\right.$$
$$\left.\left. -1 \leq \bar{u}_0 < 0, \bar{v}_0 = \sqrt{1 - \bar{u}_0^2}\right\}\right., \tag{4.4}$$

3) For $\beta = 1, \alpha \leq 1$,

$$\mathcal{CR} = \left\{(\bar{u}_0, \bar{v}_0)\left|(1-\alpha)\frac{\bar{v}_0^2}{\bar{u}_0^2}\ln\left(\frac{\rho_0}{\rho_f}\right)^2 < 1,\right.\right.$$
$$\left.\left. -1 \leq \bar{u}_0 < 0, \bar{v}_0 = \sqrt{1 - \bar{u}_0^2}\right\}\right. . \tag{4.5}$$

For all the above three cases, the LOS turn rate at t_f is

$$\|\Omega_f\| = \|\Omega_0\|\left(\frac{\rho_f}{\rho_0}\right)^{\beta-2}. \tag{4.6}$$

Proof: The procedures are similar to those given in [14] and hence are omitted here. ■

B. Bounded a_M and Known a_T

Now we consider the case when target acceleration, a_T, is known, that is,

$$A_M = a_T + \alpha v^2 e_r - \beta uve_t, \tag{4.7}$$

and both target and missile are subject to the constraint of bounded maneuverability (acceleration),

$$a_T = \text{sat}_I[A_T] = \sum_{i=r,t,\Omega} \text{sat}_{(a_{Ti\min}, a_{Ti\max})}(A_{Ti})e_i,$$
$$a_M = \text{sat}_M[A_M] = \kappa \sum_{i=r,t,\Omega} A_{Mi}e_i,$$

where

$$A_{Mr} = a_{Tr} + \alpha v^2, A_{Mt} = a_{Tt} - \beta uv, A_{M\Omega} = a_{T\Omega}.$$

Hence, the normalized missile commanded acceleration is

$$\bar{A}_{Mr} = \bar{a}_{Tr} + \alpha\bar{v}^2, \bar{A}_{Mt} = \bar{a}_{Tt} - \beta\bar{u}\bar{v}, \bar{A}_{M\Omega} = \bar{a}_{T\Omega}. \tag{4.8}$$

and the corresponding magnitude is

$$\|\bar{A}_M\| = \sqrt{(\bar{a}_{Tr} + \alpha\bar{v}^2)^2 + (\bar{a}_{Tt} - \beta\bar{u}\bar{v})^2 + \bar{a}_{T\Omega}^2}, \\ > \|\bar{a}_T\|, \text{ if } \bar{u} < 0. \tag{4.9}$$

In this section, we assume that $\beta \geq 1$, unless otherwise stated.

At first, for comparison, we consider nonmaneuvering target, that is $\bar{a}_T = 0$. In this case, the magnitude of the missile commanded acceleration is $\|\bar{A}_M\| = \bar{v}\sqrt{\beta^2\bar{u}^2 + \alpha^2\bar{v}^2}$, which renders the scaling factor $\kappa = \min(1, \frac{\|\bar{a}_M\|_{\max}}{\bar{v}\sqrt{\beta^2\bar{u}^2+\alpha^2\bar{v}^2}})$, and the equations of motion

$$\frac{d\bar{u}}{ds} = -\frac{1}{2}\bar{u}^2 + \bar{v}^2 - \kappa\alpha\bar{v}^2, \tag{4.10a}$$
$$\frac{d\bar{v}}{ds} = -\frac{3}{2}\bar{u}\bar{v} + \kappa\beta\bar{u}\bar{v}. \tag{4.10b}$$

Hence, as $\bar{A}_M$ saturates, the equations of motion on the $(\bar{u}, \bar{v})$-plane can be written as

$$\begin{aligned}\frac{d\bar{u}}{ds} &= -\frac{1}{2}\bar{u}^2 + \bar{v}^2 - \|\bar{a}_M\|_{\max}\frac{\alpha\bar{v}}{\sqrt{\beta^2\bar{u}^2 + \alpha^2\bar{v}^2}},\\ \frac{d\bar{v}}{ds} &= -\frac{3}{2}\bar{u}\bar{v} + \|\bar{a}_M\|_{\max}\frac{\beta\bar{u}}{\sqrt{\beta^2\bar{u}^2 + \alpha^2\bar{v}^2}}.\end{aligned} \tag{4.11}$$

We have seen that for unbounded $\|\bar{a}_M\|$, i.e. $\|\bar{a}_M\|_{\max} = \infty$, there exists only one equilibrium point $(\bar{u}_e, \bar{v}_e)_1 = (0, 0)$. While for finite $\|\bar{a}_M\|_{\max}$, and $\alpha > 0$, in addition to $(0, 0)$, there exists the second equilibrium point

$$(\bar{u}_e, \bar{v}_e)_2 = (0, \sqrt{\|\bar{a}_M\|_{\max}}),$$

inside the saturated region (i.e. $\bar{A}_M$ saturates). Note that $(\bar{u}_e, \bar{v}_e)_2$ is independent of α and β. For simplicity, we study further about the case $\alpha = \beta$.

Theorem 4.2: Consider a nonmaneuvering target, $a_T = 0$, if the missile commanded acceleration is

$$A_M = \beta\left[\dot{\rho}e_r + \rho\|\Omega\|e_t\right] \times \Omega, \tag{4.12}$$

where the navigation constant $\beta > 1$. Furthermore, assume that missile input acceleration is bounded, $\|\bar{a}_M\| \le \|\bar{a}_M\|_{\max}$. To capture target at finite t_f it is necessary and sufficient that

$$\mathcal{CR} = \left\{(\bar{u}_0, \bar{v}_0)\,\middle|\, \bar{v}_0 \le \frac{\rho_f}{\rho_0} + \frac{1}{2}\|\bar{a}_M\|_{\max}\left[1 - \left(\frac{\rho_f}{\rho_0}\right)^2\right],\ -1 \le \bar{u}_0 < 1, \bar{v}_0 = \sqrt{1 - \bar{u}_0^2}\right\}. \tag{4.13}$$

Proof: It can be shown that the trajectories in the $(\bar{u}\bar{w}, \bar{v}\bar{w}, \bar{w})$-space lie on a unit radius cylinder,

$$(\bar{u}^2 + \bar{v}^2)\bar{w}^2 = 1, \text{ or } \bar{w}^2 = \frac{1}{\bar{u}^2 + \bar{v}^2}. \tag{4.14}$$

Hence, we can deduce from $(2.12c)$ that, depending on the initial condition $(\bar{u}_0, \bar{v}_0, \bar{w}_0)$ the minimum $\bar{w}$ along a trajectory occurs at either of the following two cases

$$\bar{w}_{\min} = \begin{cases} 0, & \text{at } (\bar{u}, \bar{v}) = (-\infty, 0),\\ \frac{1}{\bar{v}_{\max}}, & \text{at } (\bar{u}, \bar{v}) = (0, \bar{v}_{\max}),\end{cases} \tag{4.15}$$

where $\bar{v}_{\max}$ is the maximum value of $\bar{v}$ if the trajectory is indeed a closed orbit (See Fig. 2). Furthermore, recall that at initial time $(s = s_0)$, $\bar{u}_0^2 + \bar{v}_0^2 = 1$, equations (4.11) can be simplified as

$$\begin{aligned}\left.\frac{d\bar{u}}{ds}\right|_{s=s_0} &= -\frac{1}{2}\bar{u}_0^2 + \bar{v}_0^2 - \|\bar{a}_M\|_{\max}\bar{v}_0,\\ \left.\frac{d\bar{v}}{ds}\right|_{s=s_0} &= -\frac{3}{2}\bar{u}_0\bar{v}_0 + \|\bar{a}_M\|_{\max}\bar{u}_0,\end{aligned} \tag{4.16}$$

for all admissible β (and $\alpha = \beta$). Surprisingly both (4.11) (when $\alpha = \beta$), and (4.16) are independent of β, which indicates that the related capture regions are the same for all the admissible β. It can be verified that, in the saturated region, each of the trajecty constitutes a closed orbit and satisfies

$$\bar{u}^2(\theta) + \bar{v}^2(\theta) = \frac{\sin(\theta) + \sqrt{\sin^2(\theta) - 2C_1\|\bar{a}_M\|_{\max}}}{2C_1},$$

where $\theta \triangleq \cos^{-1}(\bar{u}/\sqrt{\bar{u}^2 + \bar{v}^2}), C_1 \triangleq \bar{v}_0 - \frac{1}{2}\|\bar{a}_M\|_{\max}$. It follows from (4.14) and definition 2.1 that in this case a missile catpures a target if and only if $\bar{u}_0 \ne 1$ and

$$\frac{\rho_0}{\rho_f} \le \frac{1}{\bar{w}_{\min}^2} = \bar{v}^2(\frac{\pi}{2}) = \frac{1 + \sqrt{1 - 2C_1\|\bar{a}_M\|_{\max}}}{2C_1},$$

or equivalently, $\bar{v}_0 \le \frac{\rho_f}{\rho_0} + \frac{1}{2}\|\bar{a}_M\|_{\max}\left[1 - \left(\frac{\rho_f}{\rho_0}\right)^2\right]$. ■

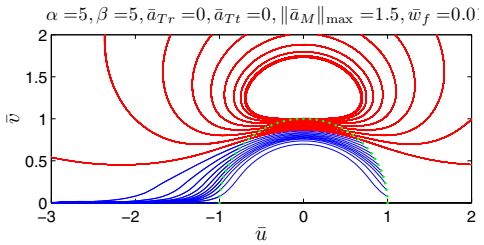

Fig. 2. State trajectories of on $(\bar{u}, \bar{v})$ plane for $\bar{a}_T = 0$, $\|\bar{a}_M\|_{\max} = 1.5$ and initial conditions $-1 \le \bar{u}_0 < 1, \bar{v}_0 = \sqrt{1 - \bar{u}_0^2}$ with $\alpha = \beta = 5$, red line: target escape, blue line: hit target

Fig. 3 illustrates the contour of capture region defined by (4.13) for different saturation level $\|\bar{a}_M\|_{\max}$ as $\bar{a}_T = 0$ and $\alpha = \beta = 5$.

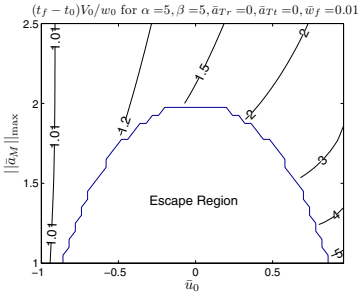

Fig. 3. The escape region (hence capture region) for various $\|\bar{a}_M\|_{\max}$ and $\alpha = \beta = 5$.

Remark 4.1: For the case of hit to kill (i.e. $\rho_f = 0$), if

$$\|\bar{a}_M\|_{\max} > 2,$$

then we have full range of capture region $-1 \le \bar{u}_0 < 0$.

For the case of $\alpha \neq \beta$, the expression of capture region is determined numerically by support vector machine in Section V.

Next, consider the case $\bar{a}_T \neq 0$. From target's aspect, it is reasonable to assume that target utilizes maximum available power to maximize $\dfrac{d\bar{u}}{ds}$ and $\dfrac{d\bar{v}}{ds}$ to escape, therefore,

$$\bar{a}_{Tr} = \bar{a}_{Tr\max}, \quad \bar{a}_{Tt} = \bar{a}_{Tt\max}, \tag{4.17}$$

and the equations of motion (2.12) can be rewritten as

$$\begin{aligned} \frac{d\bar{u}}{ds} &= -\frac{1}{2}\bar{u}^2 + \bar{v}^2 + \bar{a}_{Tr_{\max}} - \kappa(\bar{a}_{Tr_{\max}} + \alpha\bar{v}^2), \\ \frac{d\bar{v}}{ds} &= -\frac{3}{2}\bar{u}\bar{v} + \bar{a}_{Tt_{\max}} - \kappa(\bar{a}_{Tt_{\max}} - \beta\bar{u}\bar{v}). \end{aligned} \tag{4.18}$$

Equations (4.18) are highly nonlinear, the exact capture region can only be determined graphically at this moment. We will resort to support vector machine.

C. Bounded a_M and a_T with Unknown a_T

Now let's consider the case when the target acceleration, a_T, can not be obtained, and is bounded. The equations of motion for this case are

$$\begin{aligned} \frac{d\bar{u}}{ds} &= -\frac{1}{2}\bar{u}^2 + \bar{v}^2 + \bar{a}_{Tr_{\max}} - \kappa\alpha\bar{v}^2, \\ \frac{d\bar{v}}{ds} &= -\frac{3}{2}\bar{u}\bar{v} + \bar{a}_{Tt_{\max}} + \kappa\beta\bar{u}\bar{v}, \end{aligned} \tag{4.19}$$

where $\kappa = \min(1, \frac{\|\bar{a}_M\|_{\max}}{\bar{v}\sqrt{\beta^2\bar{u}^2+\alpha^2\bar{v}^2}})$. Similarly, the exact capture region will be determined numerically by support vector machine later.

V. Least Square Support Vector Machine

In order to determine the expression of the contour of capture region as shown in Fig. 3, a powerful yet simple classifier, least square support vector machine (LSSVM) [12], is implemented here. Consider a given training data set $\{x_k, y_k\}_{k=1}^N$ with input data set $x_k \in \mathbb{R}^n$ and corresponding binary class labels $y_k \in \{-1, +1\}$. Let the mapping $\phi : \mathbb{R}^n \to \mathbb{R}^m$, be the feature map mapping the input space to a higher dimensional feature space. The LSSVM problem is to determine a hyperplane, $w^{\mathrm{T}}\phi(x_i) + b$ (See Fig. 4), that minimize the performance index

$$\min_{w,b,e} J(w, e) = \frac{1}{2}w^{\mathrm{T}}w + \frac{\gamma}{2}\sum_{i=1}^{N} e_i^2, \tag{5.1}$$

subject to the equality constraints

$$y_i[w^{\mathrm{T}}\phi(x_i) + b] = 1 - e_i, i = 1, \ldots, N. \tag{5.2}$$

Then the classification function is

$$f(x_i) \triangleq \mathrm{sgn}[w^{\mathrm{T}}\phi(x_i) + b]. \tag{5.3}$$

It has been shown that [12]

$$w = \lambda^{\mathrm{T}}Z, \; b = \frac{Y^{\mathrm{T}}A^{-1}\tilde{1}}{Y^{\mathrm{T}}A^{-1}Y}, \tag{5.4}$$

where $Z^{\mathrm{T}} \triangleq \begin{bmatrix} y_1\phi(x_1) & \cdots & y_N\phi(x_N) \end{bmatrix}$, and

$$\lambda = A^{-1}(\tilde{1} - bY), A^{-1} = \left(\frac{1}{\gamma}I + ZZ^{\mathrm{T}}\right)^{-1},$$

$$Y^{\mathrm{T}} \triangleq \begin{bmatrix} y_1 & \cdots & y_N \end{bmatrix}, \tilde{1}^{\mathrm{T}} \triangleq \begin{bmatrix} 1 & \cdots & 1 \end{bmatrix},$$

The nice feature of LSSVM is that it can take the advantage of the Sherman-Morrison-Woodbury (SMW) matrix identity

$$A^{-1} = \gamma\left[I - Z\left(\gamma^{-1}I + Z^{\mathrm{T}}Z\right)^{-1}Z^{\mathrm{T}}\right], \tag{5.5}$$

so that the computational speed can be increased dramatically. However, this also makes LSSVM inevitable to compute with the feature map, $\phi(\cdot)$, although it is usually unnecessary to do so for other SVM schemes. For the determination of capture region problem, we decide to adopt the Gaussian radial basis function as the kernel function

$$K(x_i, x_j) = e^{-\frac{x_i \;\; x_j}{2\sigma^2}^2} = \phi^{\mathrm{T}}(x_i)\phi(x_j),$$

where σ is a preselected value. For this particular kernel function, the feature space is infinite dimensional, hence Taylor's series expansion are utilized to obtain the finite dimensional approximation,

$$\phi^{\mathrm{T}}(x_i)\phi(x_j) \approx \frac{\sum_{k=1}^{N_a} \frac{1}{k!}\left(\frac{x_i^{\mathrm{T}}x_j}{\sigma^2}\right)^k}{\sum_{k=1}^{N_a} \frac{1}{k!}\left(\frac{\|x_i\|^2}{2\sigma^2}\right)^k \cdot \sum_{k=1}^{N_a} \frac{1}{k!}\left(\frac{\|x_j\|^2}{2\sigma^2}\right)^k},$$

where N_a is the order of approximation. Note that in order to have better classification result, we may need to rescale the training and testing data. Once the feature mapping $\phi(\cdot)$ and the orientation of hyperplane, w, are determined, they can be stored in fighter's onboard computer to inform pilot when to release missile in real time.

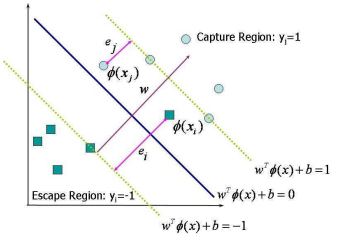

Fig. 4. Nonlinear Classification

VI. Numerical Results

In the following examples, we choose $N_a = 9, \sigma = 0.3, \bar{w}_f = 0.01$. Fig. 5-7 show the level contour of multiplier λ and the classification results for different α, β and target maneuvering levels. Owing to the space limitation, only three cases are illustrated here. For all the cases we have tried, the false classifications are less than 1%, which indicates that the technique of using the approximation of the kernel function, $K(\cdot, \cdot)$, to obtain the feature mapping $\phi(\cdot)$ is adequate for the determination of capture region. Furthermore, the variation of α (i.e. $\alpha \neq \beta$) induces the variation of capture region, not knowing target acceleration reduces the area of capture region. These observations agree with those found by Yuan [13].

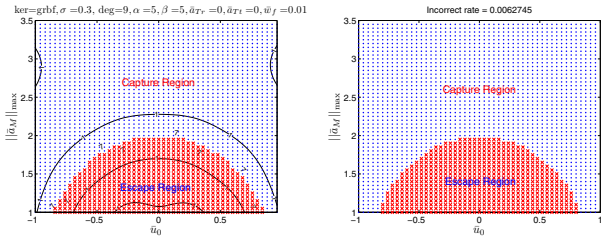

Fig. 5. For $\alpha = 5, \beta = 5, a_{Tr} = 0, a_{Tt} = 0, \bar{w}_f = 0.01$,
(Left) "·": target captured, "×": target escape, (Right) classification result

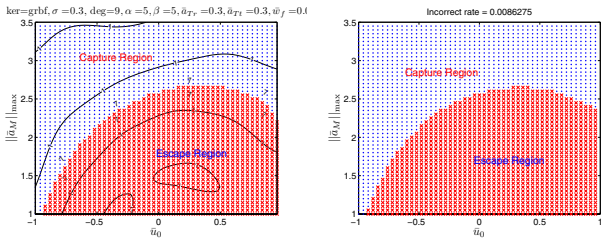

Fig. 6. For $\alpha = 5, \beta = 5, \bar{a}_{Tr} = 0.3, \bar{a}_{Tt} = 0.3$, a_T is known
(Left) "·": target captured, "×": target escape, (Right) classification result

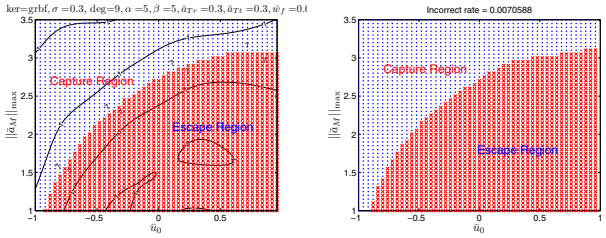

Fig. 7. For $\alpha = 5, \beta = 5, \bar{a}_{Tr} = 0.3, \bar{a}_{Tt} = 0.3$, a_T is not known.
(Left) "·": target captured, "×": target escape, (Right) classification result

VII. Conclusion

In this work, all the analysis of the relative dynamics between missile and target are performed in a LOS fixed natural coordinate. To have the capture region ready for LSSVM and visualization (in two dimensional space), all the state variables are transformed into the form of modified polar variables (MPVs). In addition, to reduce the number of independent variables, these modified polar variables are further non-dimensionalized. Then the capture region of the GIPN missile guidance law is determined by the LSSVM. However, to let LSSVM take the advantage of the Sherman-Morrison-Woodbury (SMW) matrix identity, the nonlinear feature mapping function is required. Here, a Taylor's series approximation of the Gaussian radial basis function is adopted for obtaining the related feature mapping function. From the numerical examples we have tried, a ninth order approximation of Gaussian radial basis function along with the chosen parameter yields satisfactory results. This shows that the proposed technique is suitable for expression of the capture region.

References

[1] E. Duflos, P. Penel, and P. Vanheeghe, "3D Guidance Law Modeling," *IEEE Transactions on Aerospace and Electronics Systems*, vol. 35, no. 1, pp. 72–83, January 1999.

[2] I.-J. Ha, J.-S. Hur, M.-S. Ko, and T.-L. Song, "Performance analysis of PNG laws for randomly maneuvering targets," *IEEE Transactions on Aerospace and Electronic Systems*, vol. 26, no. 5, pp. 713–720, September 1990.

[3] S.-H. Song and I.-J. Ha, "A Lyapunov-like approach to performance analysis of 3-dimensional pure PNG laws," *IEEE Transactions on Aerospace and Electronic Systems*, vol. 30, no. 1, pp. 238–247, January 1994.

[4] D. Ghose, "True proportional navigation with maneuvering target," *IEEE Transactions on Aerospace and Electronic Systems*, vol. 30, no. 1, pp. 229–237, January 1994.

[5] P.-J. Yuan and S.-C. Hsu, "Solutions of generalized proportional navigation with maneuvering and nonmaneuvering target," *IEEE Transactions on Aerospace and Electronic Systems*, vol. 31, no. 1, pp. 1–6, January 1995.

[6] A. Chakravarthy and D. Ghose, "Capturability of realistic generalized true proportional navigation," *IEEE Transactions on Aerospace and Electronic Systems*, vol. 32, no. 1, pp. 407–418, January 1996.

[7] S. N. Ghawghawe and D. Ghose, "Pure proportional navigation against time-varying target maneuvers," *IEEE Transactions on Aerospace and Electronic Systems*, vol. 32, no. 4, pp. 1336–1347, October 1996.

[8] C.-D. Yang and C.-C. Yang, "Analytical solution of 3d true proportional navigation," *IEEE Transactions on Aerospace and Electronic Systems*, vol. 32, no. 4, pp. 1509–1522, October 1996.

[9] J.-H. Oh and I.-J. Ha, "Capturability of the 3-dimensional pure png law," *IEEE Transactions on Aerospace and Electronic Systems*, vol. 35, no. 2, pp. 491–502, April 1999.

[10] F. Tyan, "The capture region of a general 3d tpn guidance law for missiles and targets with limited maneuverability," in *Proceedings of American Control Conference*, Arlington, Virginia, U. S. A., June 2001, pp. 512–517.

[11] V. N. Vapnik, *The nature of statistical learning theory*. New York, NY, USA: Springer-Verlag New York, Inc., 1995.

[12] K. S. Chua, "Efficient computations for large least square support vector machines classifiers," *Pattern Recognition Letters*, vol. 24, pp. 75–80, 2003.

[13] P.-J. Yuan, M.-G. Chen, and J.-S. Chern, "Generalized ideal proportional navigation," in *Proceedings of SPIE*, M. K. Masten and L. A. Stockum, Eds., vol. 3692, 1999.

[14] F. Tyan, "Unified approach to missile guidance laws: A 3d extension," *IEEE Transactions on Aerospace and Electronic Systems*, vol. 41, no. 4, pp. 1178–1199, October 2005.